

## Mobility of conduction electrons in ultrathin Fe and Cu films on Si(111)

D. V. Fedorov,<sup>1</sup> G. Fahsold,<sup>2</sup> A. Pucci,<sup>2</sup> P. Zahn,<sup>1</sup> and I. Mertig<sup>1</sup>

<sup>1</sup>Fachgruppe Theoretische Physik, Fachbereich Physik, Martin-Luther-Universität Halle-Wittenberg, D-06099 Halle, Germany

<sup>2</sup>Kirchhoff-Institut für Physik der Ruprecht-Karls-Universität Heidelberg, Im Neuenheimer Feld 227, D-69120 Heidelberg, Germany

(Received 7 March 2007; published 21 June 2007)

Using *in situ* transmission spectroscopy in the middle infrared, an enhancement of the Drude-type plasma frequency with respect to the bulk value was found for ultrathin Fe films in  $\langle 111 \rangle$  orientation grown on Si(111) $7 \times 7$ . That finding is in good agreement with *ab initio* calculations that, in particular, take into account the existence of surface states and surface resonances. These calculations also predict an increase of the plasma frequency with decreasing thickness for Cu(111) films, but the experimental proof for Cu was hampered by an islandlike growth. However, in experiment and in theory the bulk value for the plasma frequency of copper is already reached at 3 nm thickness.

DOI: [10.1103/PhysRevB.75.245427](https://doi.org/10.1103/PhysRevB.75.245427)

PACS number(s): 73.20.At, 73.50.-h, 78.20.-e, 78.67.-n

### I. INTRODUCTION

Transport properties of ultrathin metallic films are of basic interest for the development of nanoscaled electronic devices. The properties of ultrathin films with a thickness of a few atomic layers are determined to a large extent by the surfaces and interfaces. In addition to the change of the local properties at the boundaries, quantum confinement effects cause oscillations of macroscopic properties, such as the magnetic interlayer exchange coupling<sup>1</sup> and specifically the electrical conductivity.<sup>2,3</sup> Thus, the properties of nanostructures can substantially differ from bulk properties. Within the relaxation time approximation, features of the plasma frequency can be transferred to the interpretation of the charge carrier mobility in thin films. The electrical conductivity can be strongly decreased due to surface scattering. Nevertheless, under certain circumstances, if the size- and surface-dependent band structure results in an increased plasma frequency, conductivity of ultrathin films can be increased with respect to bulk values.

In this paper, we study candidates for increased conductivity. We compare the results from infrared (IR) transmittance spectroscopy as a noncontact measurement of the film plasma frequency with results obtained by *ab initio* calculations. This provides insight into the character of the valence electrons and related consequences for the carrier mobility. The obtained results are qualitatively different to the well-known behavior found for the parabolic-band model where the conductivity strongly decreases with decreasing thickness.<sup>4</sup> Using *ab initio* calculations of the plasma frequency, we explain the discrepancy by the changes of the electronic structure at surfaces and interfaces, which was not taken into account in models with thickness-independent dispersion.

For the experimental studies Fe and Cu, respectively, were deposited onto Si(111). For this substrate, the formation of (111) film surfaces was proved.<sup>5,6</sup> To avoid intermixing at the interface, the substrates were cooled during deposition. In contrast to Fe on Si(100), silicide interlayer formation was not observed for iron on Si(111), not even at room temperature. The growth of Fe on Si(111) starts with the formation of a pseudomorphic layer that relaxes with increasing film

thickness above 1 nm.<sup>6</sup> For Cu growth on Si(111), it is known that silicide is formed at the interface.<sup>7,8</sup> The interlayer formation needs reactive Si atoms and, therefore, should be favored by stepped surfaces.<sup>9</sup> In Refs. 7–9, the interlayer thickness at room temperature and below is mentioned to be one to a few monolayers. The interlayer plays a key role in overcoming the large lattice mismatch between Cu and Si.<sup>7</sup> On top of the interlayer, a pure Cu film is formed, but the growth is not an ideal layer-by-layer one,<sup>8</sup> which gives film roughness at the beginning of that growth phase. In the case of room temperature growth, smooth Cu(111) films were found already at about 3 nm thickness. Their  $p(1 \times 1)$  low-energy electron diffraction (LEED) pattern was rotated by  $30^\circ$  with respect to the Si substrate, indicating the fcc arrangement of the Cu atoms.<sup>10</sup>

### II. EXPERIMENT

The *in situ* experiments were performed with a vacuum Fourier-transform IR spectrometer (Bruker IFS 66 v/S with midrange mercury cadmium telluride detector) attached to an ultrahigh vacuum (UHV) chamber (base pressure  $< 2 \times 10^{-8}$  Pa). A LEED system allows for *in situ* characterization of the crystalline quality of surfaces and films. The preparation of the Si(111) substrates was as follows: For the Fe film, the silicon wafer was heated to 1300 K for 20 min in UHV to desorb the oxide, which revealed a clear  $(7 \times 7)$  LEED pattern after cooling. For the Cu-film series that is discussed here, we used high resistivity hydrogen terminated *n*-type Si and thermally processed it under UHV by heating to 1130 K for 1 min. Because of the rather rapid cooling and relatively low heating temperature, a perfect  $(7 \times 7)$  superstructure was not obtained. However, as we know from various growth experiments at about 100 K, this kind of substrate surface gave Cu films with lower scattering rate at about 5 nm thickness than films grown on the perfect  $(7 \times 7)$  superstructure.

The metals were deposited with an Omicron electron impact evaporator at an angle of incidence of about  $35^\circ$ . Metal-film thicknesses are calculated from the deposition time and the rate (typically 0.1–0.2 nm/min assuming bulk density) that was calibrated with a quartz microbalance, which results

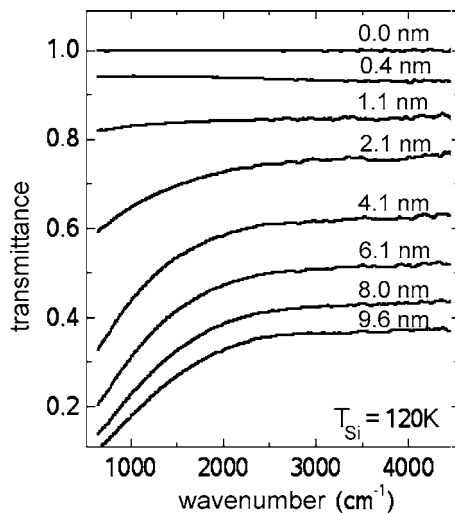


FIG. 1. Selection of transmittance spectra (normal incidence, spectra divided by the transmittance of the substrate) measured for Fe growing on Si(111) at 120 K. Unity means the same transmittance as the substrate and the labels indicate the average film thickness. Drude-type fits to the spectra give reasonable values from 0 nm thickness.

in a relative error of about 10%. From the bulk structure, it follows in monolayers (ML) that along the  $\langle 111 \rangle$  direction 1 ML=0.083 nm for Fe and 1 ML=0.208 nm for Cu. Substrate temperatures were measured by a Chromel-Alumel thermocouple attached to the sample holder. They were 120 K for Fe deposition and 102 K for Cu deposition, respectively. After metal deposition, the crystalline film structure was investigated with LEED. For Fe with 10 nm thickness, we observed patterns corresponding to the  $\langle 111 \rangle$  film orientation. For the Cu films with 5 nm thickness, only a circle with increased diffraction intensity characteristic for  $\langle 111 \rangle$  orientation was observed. During metal deposition, the IR transmittance at normal incidence was recorded (spectral resolution of 32  $\text{cm}^{-1}$ , 100 scans accumulated within 22 s). A selection of spectra is presented in Figs. 1 and 2.

The spectra were analyzed with a Drude-type model for the dielectric function (of the circular frequency  $\omega$ ),

$$\epsilon(\omega) = 1 - \frac{\omega_p^2}{\omega(\omega + i\omega_r)}, \quad (1)$$

with the scattering rate

$$\omega_r(\omega, d) = \omega_s(d) + \omega_{\tau, \text{bulk}}(\omega) \quad (2)$$

as a superposition of a surface contribution  $\omega_s(d)$  (that depends on film thickness  $d$  and film roughness) and of the frequency-dependent bulk scattering rate,<sup>11-13</sup>

$$\omega_{\tau, \text{bulk}}(\omega) = \omega_{\tau 0} + \gamma\omega^2. \quad (3)$$

The parameters of the frequency-dependent bulk scattering rate are determined by a fit to the bulk data for the optical and dc properties at different temperatures.<sup>11,12</sup> The optical data were taken from Ref. 14. As in this reference, regarding the large values of the negative real part of  $\epsilon(\omega)$ , any background susceptibility is set to zero. The bulk optical data,

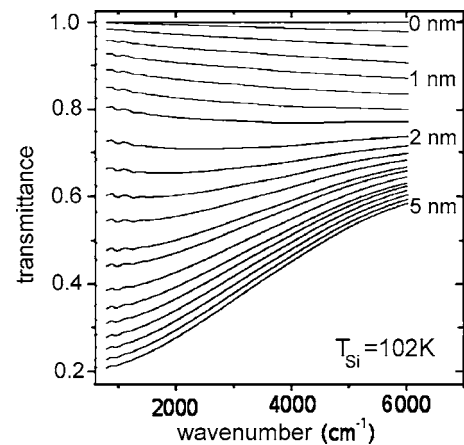


FIG. 2. Selection of transmittance spectra (normal incidence spectra divided by the transmittance of the substrate) measured for Cu on Si(111) at 102 K. Unity means the same transmittance as the substrate. Spectra are shown in steps of 0.25 nm in average film thickness (indicated only for some of the spectra). Drude-type fits to the spectra are performed for thicknesses from 2 nm.

especially the dispersion of the imaginary part  $\text{Im}[\epsilon(\omega)]$ , reveal Drude-type behavior of Fe and Cu in the mid-IR range. The onset of interband transitions is indicated by an increase or at least a plateau in  $\text{Im}[\epsilon(\omega)]$ . This occurs well above wave numbers of 6000  $\text{cm}^{-1}$  for Fe and above 12 000  $\text{cm}^{-1}$  for Cu. The film plasma frequency is assumed to be proportional to the bulk values:

$$\omega_{P, \text{film}}(\omega, d) = \beta(d)\omega_{P, \text{bulk}}(\omega). \quad (4)$$

The functions  $\beta(d)$  and  $\omega_s(d)$  are used as parameters in the spectral fits that were done from 1000 to 4500  $\text{cm}^{-1}$  and from 600 to 5500  $\text{cm}^{-1}$  for Cu and Fe, respectively.

In the beginning of Fe growth, there is an extraordinary strong decrease in transmittance, significantly stronger than the one calculated with bulk values. This indicates an increased metallic conductivity. The slope in iron-film spectra for low thicknesses reflects the strong frequency dependence of the Drude parameters of the bulk.<sup>11</sup> For all thicknesses, the Fe-film spectra can be perfectly fitted with reasonable Drude parameters. As a result, the Fe-surface roughness as shown in Fig. 3 increases up to 1 nm and then it saturates in accordance to Fig. 2 of Ref. 6. Figure 3 shows  $\omega_s(d)$  for Cu and Fe films scaled by the film thickness and the bulk Fermi velocity  $v_F$ . The almost constant values of this parameter for large thicknesses point to thickness-independent diffuse surface scattering<sup>15</sup> as described in the classical size effect by the theory of Fuchs and Sondheimer.<sup>16,17</sup>

For Cu below 2 nm thickness, a negative transmittance-curve slope, that is, transmittance decreases with increasing wave number, indicates a significant deviation from the metallic layer's dispersion. The dispersion is typical for flat metal islands that have their absorption maximum beyond the mid IR. The metal-island-like dispersion starts already at a deposition of about 1 ML, which means that any silicide layer must be very thin. The coalescence of copper islands reaches the percolation threshold at about 2 nm. Therefore,

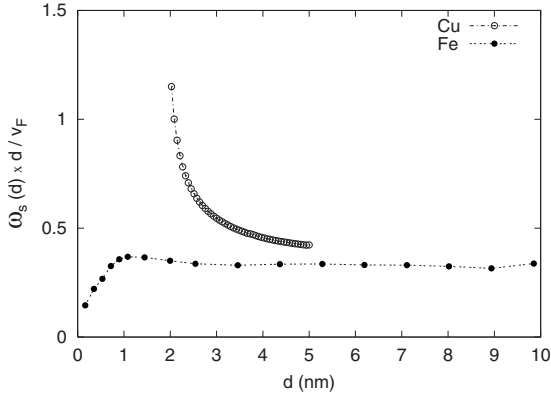


FIG. 3. The thickness dependence of the surface contribution to the scattering rate for Cu/Si(111) and Fe/Si(111).

the fitting procedure was performed for Cu only for thicknesses above 2 nm.

The square of  $\beta(d)$  will be compared to our theoretical calculations (see Figs. 4 and 5).

### III. THEORY

Within the quasiclassical approach, the tensor of the squared plasma frequency  $\hat{\omega}_p^2$  is connected with the effective mass tensor  $\hat{M}(k)$ :<sup>18</sup>

$$\hat{\omega}_p^2 = \frac{4\pi e^2}{V} \sum_k f^0(E_k) [\hat{M}(k)]^{-1}, \quad (5)$$

where  $e$  is the electron charge,  $V$  the system volume,  $f^0(E_k)$  the Fermi-Dirac occupation function in the limit of zero temperature, and  $E_k$  the energy of an electron (here  $k$  is a shorthand notation for crystal momentum vector  $\mathbf{k}$  and band index  $n$ ). In the isotropic relaxation time approximation [see, for instance, Eq. (13.27) in Ref. 19], the plasma frequency can be related to the conductivity  $\sigma$  and the relaxation time  $\tau$  similar to the Drude model:  $\omega_p^2 = 4\pi\sigma/\tau$ . Therefore, according to Refs. 20–22, we can write for the plasma frequency (per spin direction  $\sigma$ ) the following expression:

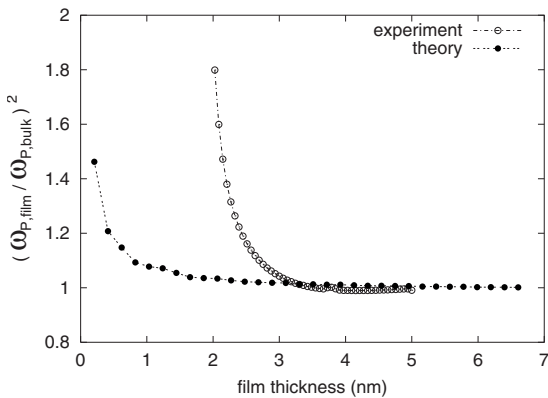


FIG. 4. Experimental data and theoretical results of the film plasma frequency  $\omega_{p,\text{film}}$  relative to the bulk value  $\omega_{p,\text{bulk}}$  for Cu/Si(111).

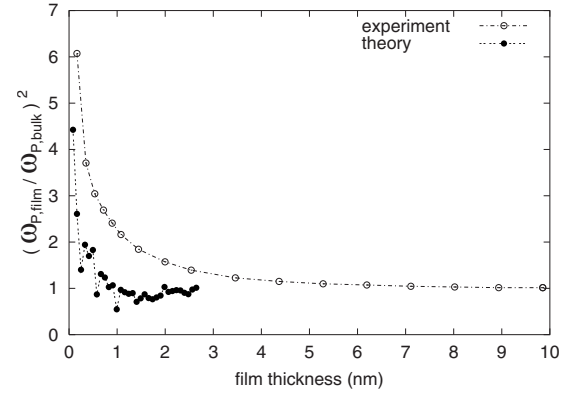


FIG. 5. Experimental data and theoretical results of the film plasma frequency  $\omega_{p,\text{film}}$  relative to the bulk value  $\omega_{p,\text{bulk}}$  for Fe/Si(111).

$$(\omega_p^\sigma)^2 = \frac{4\pi e^2}{V} \sum_k \delta(E_k^\sigma - E_F) v_{k,i}^\sigma v_{k,i}^\sigma, \quad (6)$$

where  $E_F$  is the Fermi energy, and  $v_{k,i}^\sigma$  denotes one Cartesian component of the group velocity vector  $\mathbf{v}_k^\sigma$ . Here, we exploit the fact that for a cubic crystal or a two-dimensional lattice with  $C_{4v}$  or  $C_{6v}$  symmetry, the conductivity tensor is isotropic and is represented by a scalar.

Finally, performing the integration in Eq. (6) over the Fermi surface, we obtain in the case of a bulk system

$$(\omega_{p,\text{bulk}}^\sigma)^2 = \frac{e^2}{2\pi^2 \hbar} \oint_{E_k^\sigma = E_F} \frac{dS_k^\sigma}{|\mathbf{v}_k^\sigma|} v_{k,i}^\sigma v_{k,i}^\sigma, \quad (7)$$

where  $dS_k^\sigma$  is a differential Fermi surface element of the  $n$ th Fermi surface sheet.

In the case of a film with the thickness  $d$ , performing the integration in Eq. (6) over the Fermi lines, we can rewrite the expression for the spin-dependent plasma frequency in the following form:

$$(\omega_{p,\text{film}}^\sigma)^2 = \frac{e^2}{\pi \hbar d} \oint_{E_k^\sigma = E_F} \frac{dl_k^\sigma}{|\mathbf{v}_k^\sigma|} v_{k,i}^\sigma v_{k,i}^\sigma, \quad (8)$$

where  $dl_k^\sigma$  is a differential Fermi line element arising from the  $n$ th band.

The electronic structure of the considered systems was calculated self-consistently using a screened Kohn-Rostoker multiple scattering Green's function method.<sup>23–27</sup> Spherical potentials in the atomic sphere approximation were used and an angular momentum expansion of the charge density up to  $l_{\text{max}}=6$  was used. Exchange and correlation effects were included within the local-density approximation in the parametrization of Vosko *et al.*<sup>28</sup> The film unit cell contains  $N$  atoms of the considered material, each representing one atomic layer and sufficient empty sites on both sides of the film to ensure a proper treatment of the charge relaxation at the surfaces. Structural surface relaxations were not taken into account. However, in experiment the films are deposited on a substrate and the electronic structure at the interface is different from the idealized one. The modeling of the realistic interface structure is out of the scope of these investiga-

tions. Due to the slab geometry, the states at the Fermi level are described by lines in the two-dimensional Brillouin zone (BZ). The Fermi surface integrals have to be replaced by line integrals according to Eq. (8).<sup>29</sup> In the considered (111) surface geometry, the irreducible part equals one twelfth of the whole BZ and contains about 100 000  $\mathbf{k}_{\parallel}$  points to obtain convergence of the transport integral in Eq. (8).

#### IV. RESULTS

The plasma frequencies of Cu(111) and Fe(111) films in the thickness range of 2–5 nm and 0–10 nm, respectively, from Drude fits to IR transmittance spectra were compared to theoretical results for Cu(111) and Fe(111) slabs in the thickness range between 1 and 32 ML. The theoretically treated thicknesses correspond to about 0.2–6.6 nm for Cu(111), and about 0.1–2.6 nm for Fe(111) films.

Figure 4 shows the experimental and theoretical results for  $(\omega_{p,\text{film}})^2$  of Cu(111) films. Due to the fact that the Fermi surface of bulk Cu is very similar to a sphere,<sup>20</sup> a free-electron model<sup>4</sup> was used to explain the plasma frequency of Cu films. In this parabolic-band model,  $\omega_p^2$  is proportional to the charge density and vanishes with the layer thickness going to zero.<sup>4</sup> In contrast, a strong increase of  $\omega_{p,\text{film}}$  for small thicknesses is obtained from our *ab initio* calculations (Fig. 4). As it was shown in Ref. 22, the main reason of this effect is the increase of the Fermi velocity caused by the large contribution of fast surface states and resonances. In the experiment, the continuous Cu film is formed only after 2 nm average thickness. Below 3 nm, the increase in the plasma-frequency parameter partially reflects the typical behavior after percolation.<sup>11</sup> So, comparison to theory is not possible below 3 nm, but at about 3 nm, the bulk value is reached in theory and experiment, which is an important result and which may be of great interest for the production of nanointerconnects.

Bulk Fe has a complicated Fermi surface<sup>20</sup> with a few sheets for each spin direction. In this case, the applicability of the Drude-Sommerfeld approximation is restricted because of very different characters of electronic states at the Fermi level. That seems to be one reason of the limited quantitative agreement between the experimental values of  $(\omega_{p,\text{film}})^2$  and the theoretical results in Fig. 5. Another reason could be the change of the lattice constant in the pseudomorphic Fe layer below 1 nm.<sup>6</sup> Nevertheless, the significant in-

crease of the plasma frequency for small Fe thicknesses is reproduced.

In addition, our *ab initio* calculations show strong oscillations of the plasma frequency in dependence on the film thickness for very thin Fe(111) films. It is a clear quantum size effect<sup>4,30–32</sup> like the density of states oscillations in the case of Cu(001) films.<sup>22</sup> In a recent publication,<sup>33</sup> we have shown that this effect is governed by corresponding Fermi surface nesting vectors along the  $\langle 111 \rangle$  direction. In the *in situ* experiment, the thickness resolution was limited and the growth was not an ideal layer-by-layer one, which smeared out any oscillation on a small-thickness scale.

#### V. SUMMARY

We have investigated the Drude-type plasma frequency  $\omega_{p,\text{film}}$  for Cu/Si(111) and Fe/Si(111) films. The qualitative behavior of the theoretical values of the plasma frequency is very close to experimental data particularly in the case of the Fe films. It can be concluded that the method for the extraction of the plasma frequency from the experimental IR transmittance spectra is valid and can be used to analyze the mobility of conduction electrons in ultrathin metallic films and multilayers. So, the considered experimental method is well suited for the investigation of the transport properties of metallic components of nanoscaled electronic devices. However, comparison to theory may be hampered by film growth different to ideal theoretical assumptions. Our results are qualitatively different from the prediction of a free-electron model,<sup>4</sup> where the squared plasma frequency  $\omega_{p,\text{film}}^2$  vanishes with the film thickness going to zero. The calculated and observed strong increase of  $\omega_{p,\text{film}}^2$  for small thicknesses is related to the increase of the Fermi velocity caused by the large contribution of surface states and resonances. In addition, our *ab initio* calculations find a pronounced quantum size effect for very thin Fe(111) films, which is analyzed in detail in Ref. 33.

#### ACKNOWLEDGMENT

This work has been supported by the Deutsche Forschungsgemeinschaft (projects LE 736, PU 193, ME 1153/8-1, and FG 404).

<sup>1</sup>P. Grünberg, R. Schreiber, Y. Pang, M. B. Brodsky, and H. Sowers, Phys. Rev. Lett. **57**, 2442 (1986).

<sup>2</sup>M. Jałochowski, M. Hoffmann, and E. Bauer, Phys. Rev. Lett. **76**, 4227 (1996).

<sup>3</sup>I. Vilfan, M. Henzler, O. Pfennigstorf, and H. Pfnür, Phys. Rev. B **66**, 241306(R) (2002).

<sup>4</sup>N. Trivedi and N. W. Ashcroft, Phys. Rev. B **38**, 12298 (1988).

<sup>5</sup>K. Pedersen, T. B. Kristensen, T. G. Pedersen, P. Morgen, Z. Li, and S. V. Hoffmann, Phys. Rev. B **66**, 153406 (2002).

<sup>6</sup>H. J. Kim, D. Y. Noh, J. H. Je, and Y. Hwu, Phys. Rev. B **59**, 4650 (1999).

<sup>7</sup>F. J. Walker, E. D. Specht, and R. A. McKee, Phys. Rev. Lett. **67**, 2818 (1991).

<sup>8</sup>Z. H. Zhang, S. Hasegawa, and S. Ino, Surf. Sci. **415**, 363 (1998).

<sup>9</sup>R. A. Simão, C. A. Achete, and H. Niehus, J. Vac. Sci. Technol. A **15**, 1531 (1997).

<sup>10</sup>P. Castrucci, R. Gunella, R. Bernardini, M. De Crescenzi, L. Ferrari, C. Crotti, C. Comicioli, C. Ottaviani, G. Gubbiotti, and G.

- Carlotti, Surf. Sci. **476**, 43 (2001).
- <sup>11</sup>G. Fahsold, A. Bartel, O. Krauth, N. Magg, and A. Pucci, Phys. Rev. B **61**, 14108 (2000).
- <sup>12</sup>G. Fahsold, M. Sinther, A. Priebe, S. Diez, and A. Pucci, Phys. Rev. B **65**, 235408 (2002).
- <sup>13</sup>G. Fahsold, M. Sinther, A. Priebe, S. Diez, and A. Pucci, Phys. Rev. B **70**, 115406 (2004).
- <sup>14</sup>M. A. Ordal, R. J. Bell, R. W. Alexander, Jr., L. L. Long, and M. R. Querry, Appl. Opt. **24**, 4493 (1985).
- <sup>15</sup>A. Pucci, F. Kost, G. Fahsold, and M. Jałochowski, Phys. Rev. B **74**, 125428 (2006).
- <sup>16</sup>K. Fuchs, Proc. Cambridge Philos. Soc. **34**, 100 (1938).
- <sup>17</sup>E. H. Sondheimer, Adv. Phys. **1**, 1 (1952).
- <sup>18</sup>*Ergebnisse in der Elektronentheorie der Metalle*, edited by P. Ziesche and G. Lehmann (Akademie-Verlag, Berlin, 1983), p. 253.
- <sup>19</sup>N. W. Ashcroft and N. D. Mermin, *Solid State Physics* (Holt-Saunders International Editions, New York, 1976).
- <sup>20</sup>I. Mertig, Rep. Prog. Phys. **62**, 237 (1999).
- <sup>21</sup>P. Zahn, I. Mertig, M. Richter, and H. Eschrig, Phys. Rev. Lett. **75**, 2996 (1995).
- <sup>22</sup>D. V. Fedorov, P. Zahn, and I. Mertig, Thin Solid Films **473**, 346 (2005).
- <sup>23</sup>P. Zahn, J. Binder, I. Mertig, R. Zeller, and P. H. Dederichs, Phys. Rev. Lett. **80**, 4309 (1998).
- <sup>24</sup>O. K. Andersen, A. V. Postnikov, and S. Yu. Savrasov, in *Applications of Multiple Scattering Theory to Materials Science*, MRS Symposia Proceedings No. 253 (Materials Research Society, Pittsburgh, 1992), p. 37.
- <sup>25</sup>L. Szunyogh, B. Újfalussy, P. Weinberger, and J. Kollár, Phys. Rev. B **49**, 2721 (1994).
- <sup>26</sup>R. Zeller, P. H. Dederichs, B. Újfalussy, L. Szunyogh, and P. Weinberger, Phys. Rev. B **52**, 8807 (1995).
- <sup>27</sup>N. Papanikolaou, R. Zeller, and P. H. Dederichs, J. Phys.: Condens. Matter **14**, 2799 (2002).
- <sup>28</sup>S. H. Vosko, L. Wilk, and M. Nusair, Can. J. Phys. **58**, 1200 (1980).
- <sup>29</sup>P. Zahn, N. Papanikolaou, F. Erler, and I. Mertig, Phys. Rev. B **65**, 134432 (2002).
- <sup>30</sup>F. K. Schulte, Surf. Sci. **55**, 427 (1976).
- <sup>31</sup>S. Ciraci and I. P. Batra, Phys. Rev. B **33**, 4294 (1986).
- <sup>32</sup>G. Materzanini, P. Saalfrank, and P. J. D. Lindan, Phys. Rev. B **63**, 235405 (2001).
- <sup>33</sup>D. V. Fedorov, P. Zahn, and I. Mertig, Thin Solid Films **515**, 6921 (2007).